**Supplement File**

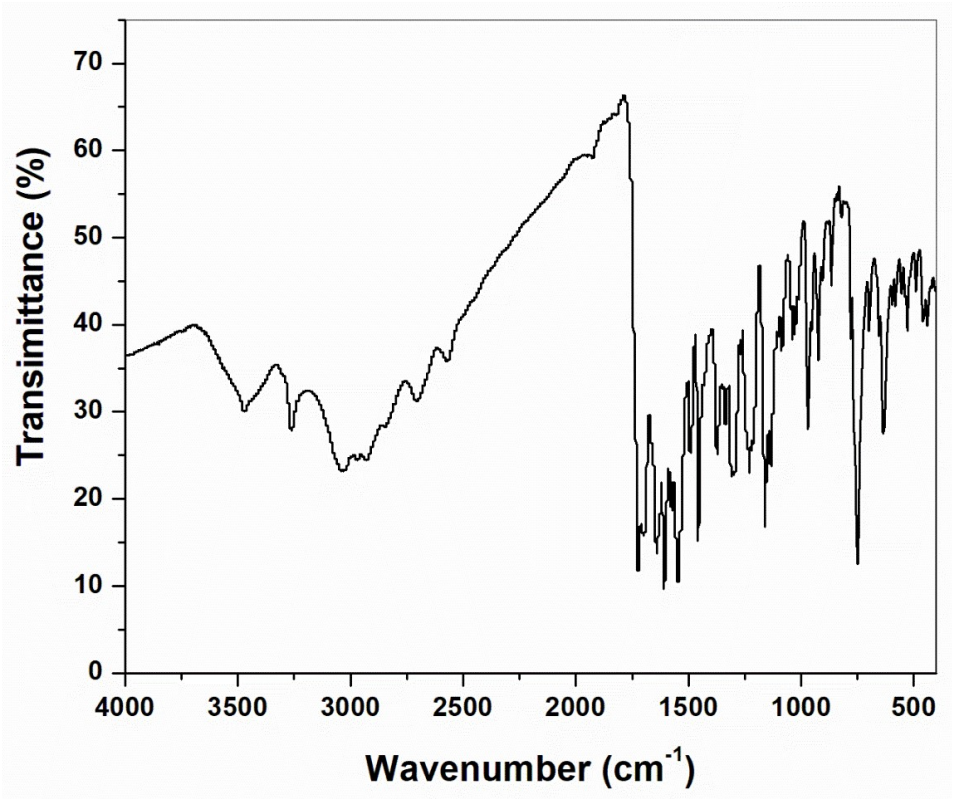


**Figure S1.** FT-IR spectrum of **HCBH**.

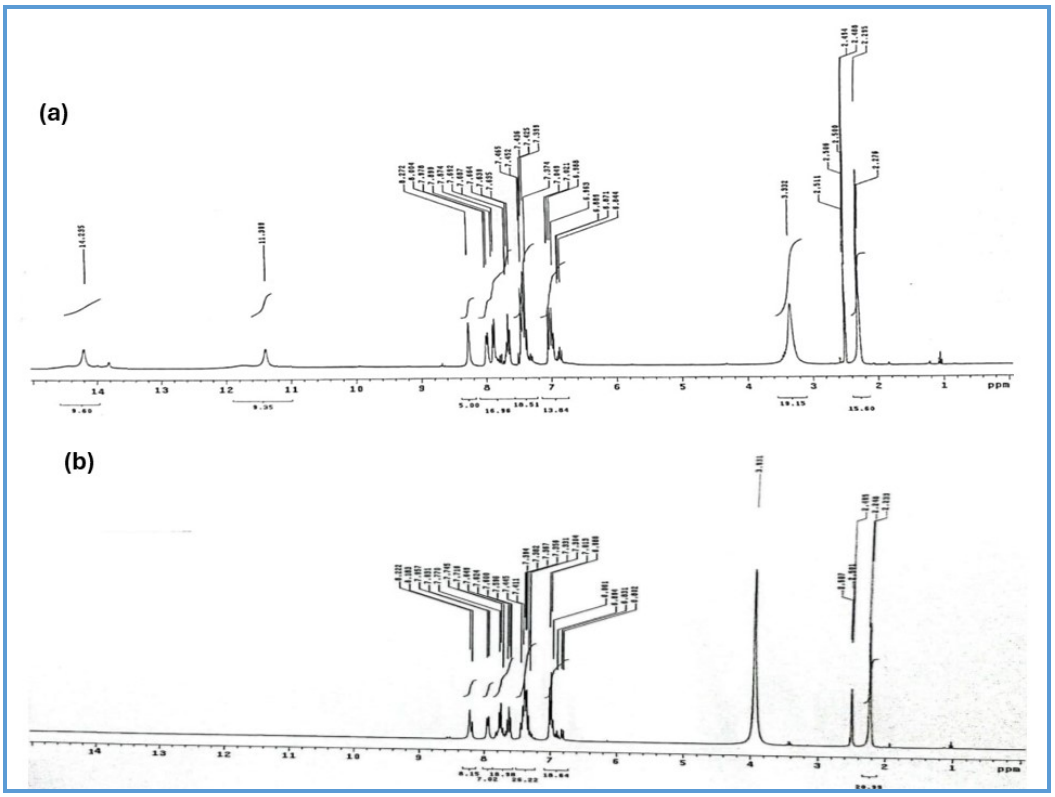


**Figure S2.** $^1$HNMR spectrum of **HCBH** (a) with DMSO (b) with DMSO/$D_2O$.

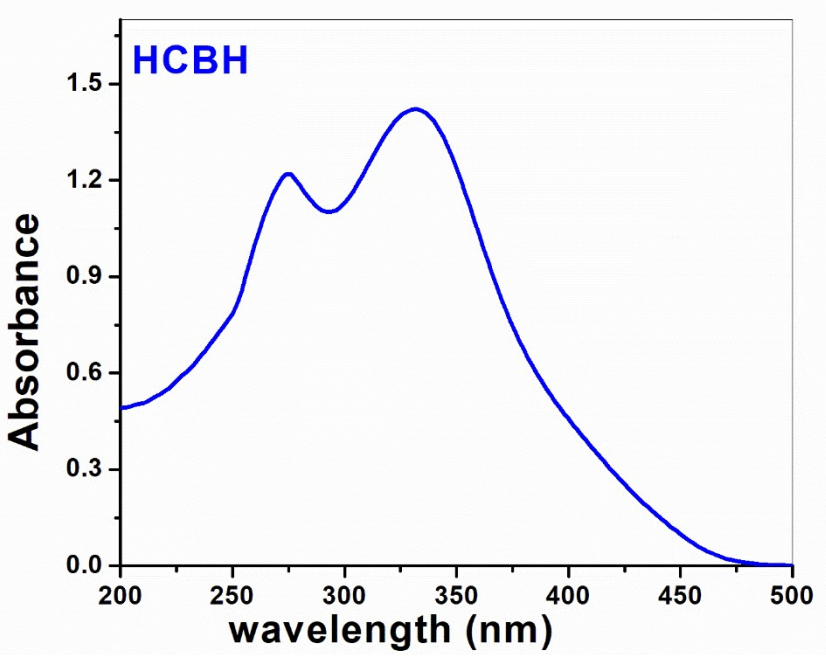


**Figure S3.** The electronic spectrum of **HCBH**

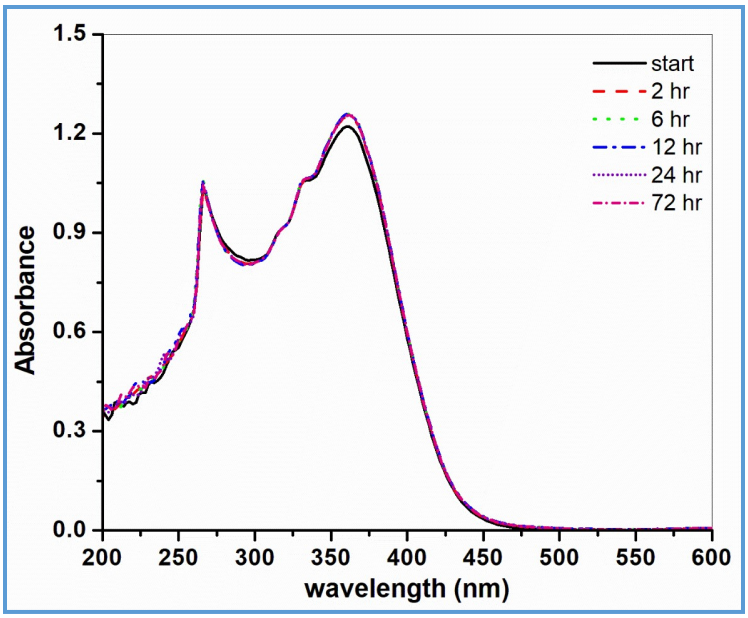


**Figure S4.** Representative time-dependent UV–vis spectra of **CuH** nano-chelate at 25 °C.

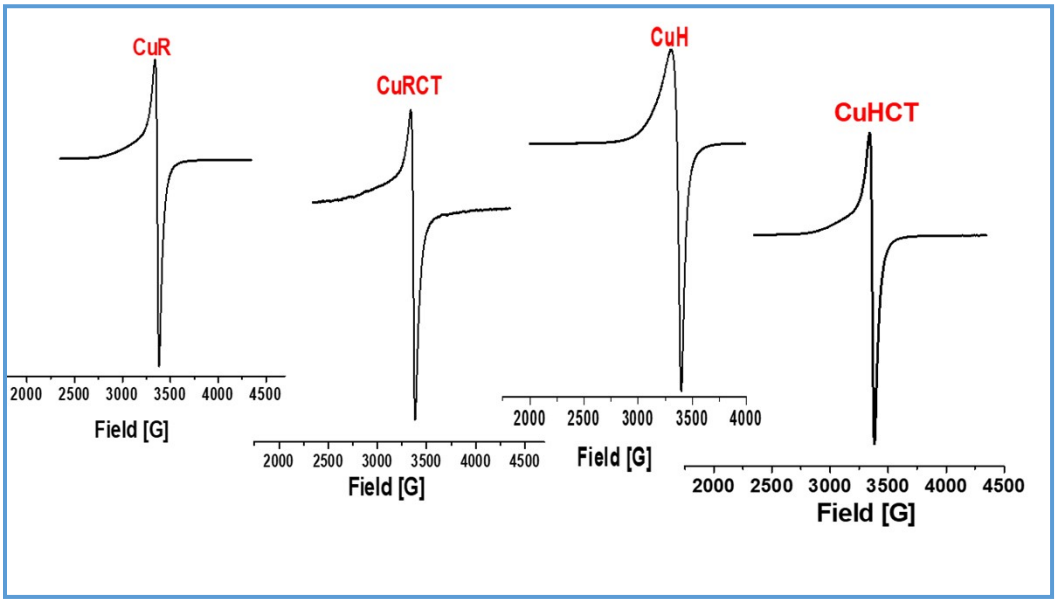


**Figure S5.** ESR spectra of **CuR**, **CuRCT**, **CuH** and **CuHCT** nano-chelates.

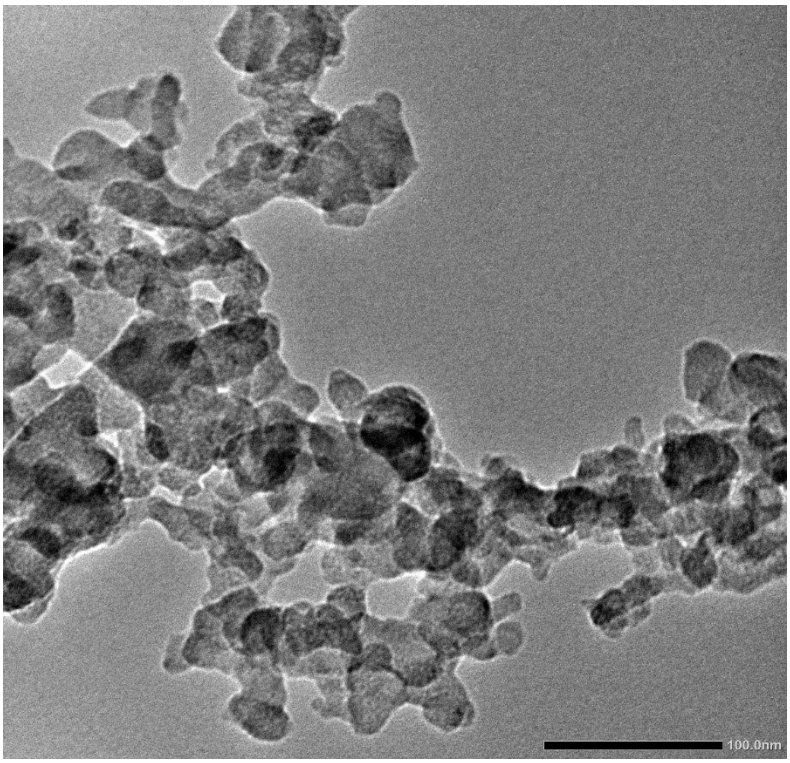


**Figure S6**. TEM image of **CuH** dispersed in silica

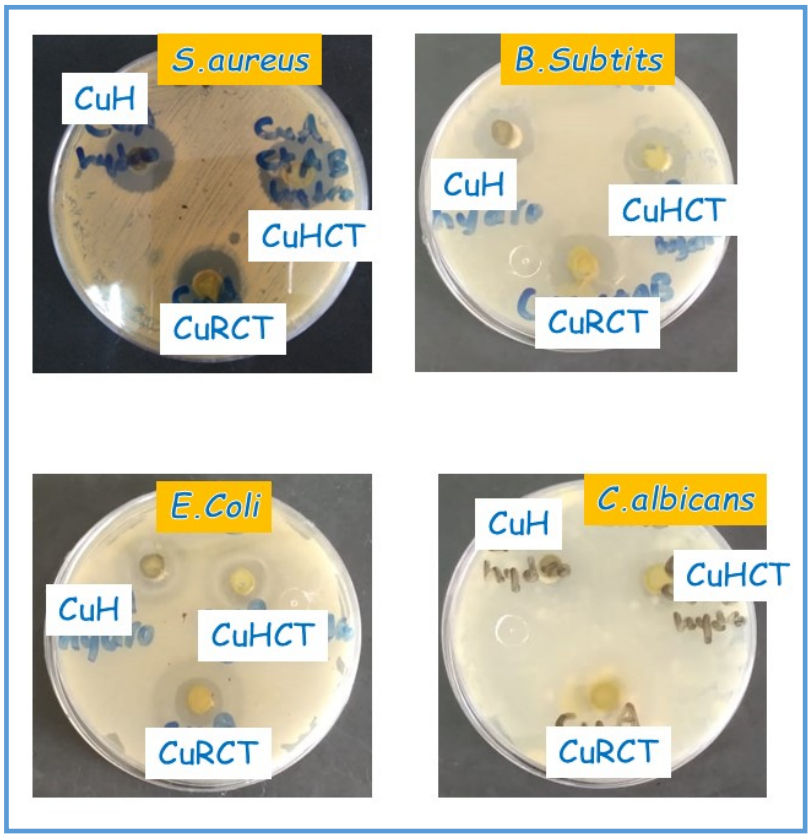

**Figure S7.** The Inhibition zone diameter of copper nano-chelates against *S. aureus, B. subtilis, E. coli*. (bacteria) and *C. albicans (fungi)*.

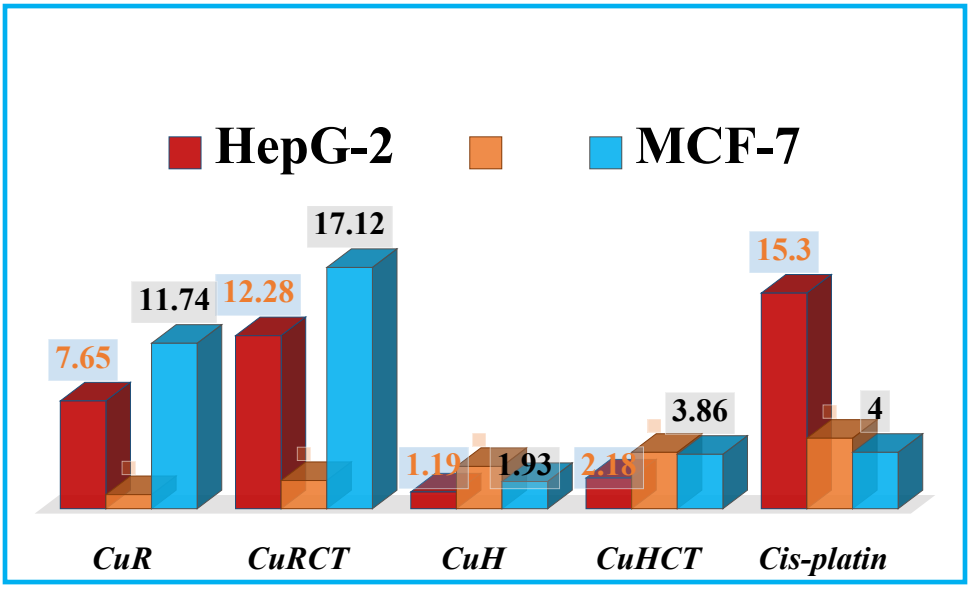


**Figure S8.** Comparison between $IC_{50}$ of **HCBH, CuR, CuRCT, CuH** and **CuHCT** nano-chelates and standard *cis-platin*.

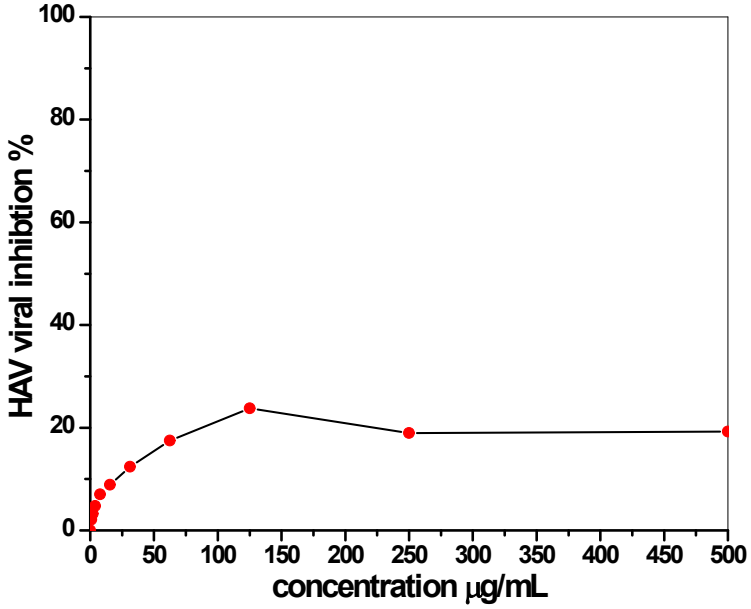


**Figure S9**. The antiviral activity of **CuH** nano-chelate against Hepatitis A virus (HAV).

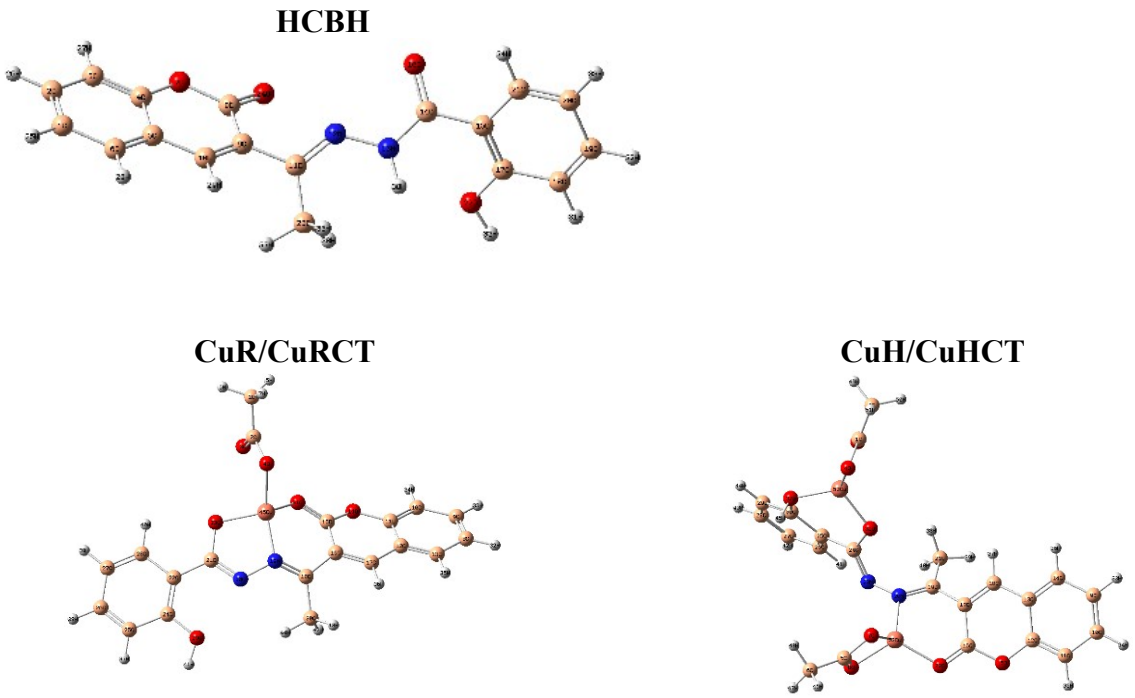


**Figure S10.** Optimized 3D structures of the **HCBH** and its copper chelates.

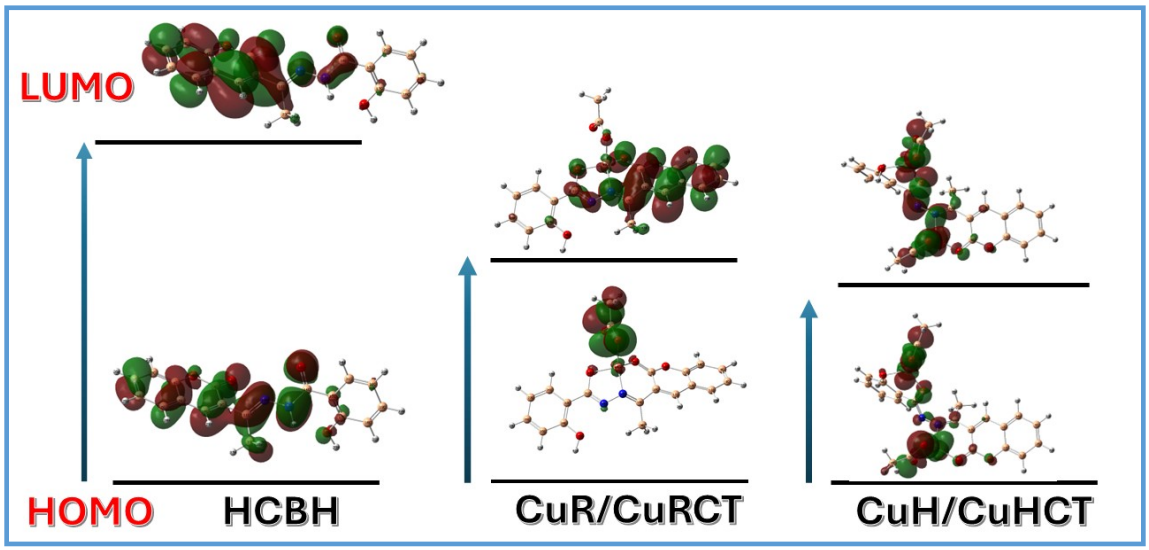


**Figure S11.** Graphical representation of HOMO-LUMO distribution of the HCBH and its copper nano-chelates.

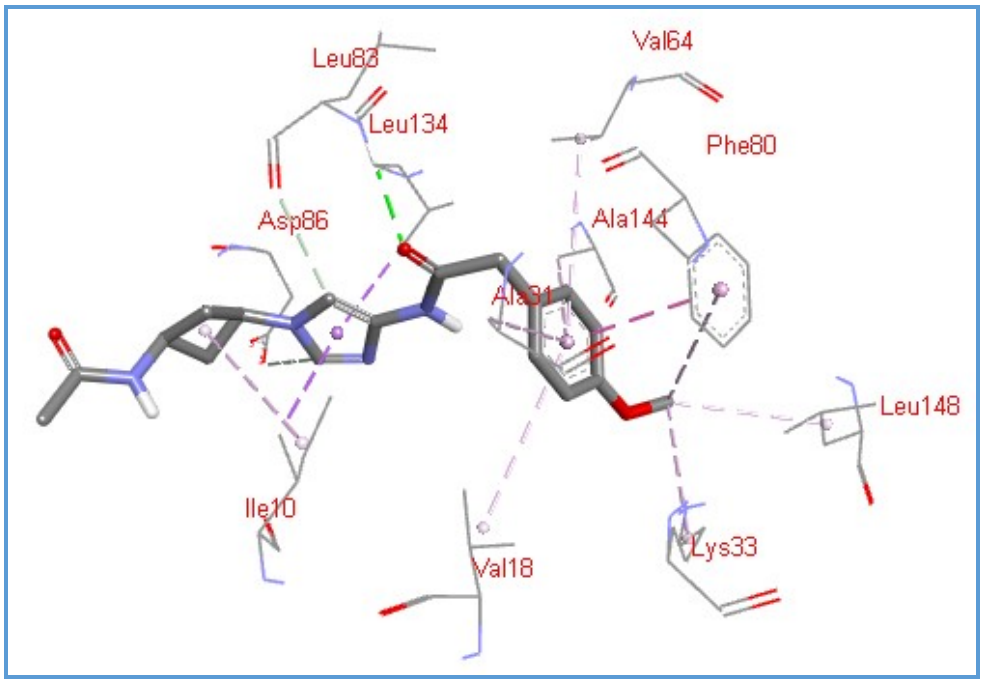


**Figure S12.** 3D representation of the (N-(1-[cis-3-(acetylamino)cyclobutyl]-1H-imidazol-4-yl)-2-(4-methoxyphenyl)acetamide ligand in target protein (pdb ID: 3IG7).

**Table S1.** Analytical, physical, and molar conductance data of the (**HCBH**) and its copper nano-chelates.

| Compound | Molecular Formula, [F.Wt] | Color | Yield (%) | M.P. (˚C) | Elemental analysis, found % (calcd %) | | | | $\Omega_m$ (ohm$^{-1}$ cm$^2$ mol$^{-1}$) |
|---|---|---|---|---|---|---|---|---|---|
| | | | | | % C | % H | % N | % M | |
| **HCBH** | $C_{18}H_{14}N_2O_4$ [322.32] | White | 92 | 229 | 67.00 (67.07) | 4.30 (4.37) | 8.55 (8.69) | - | - |
| **CuR** | $C_{20}H_{16}N_2O_6Cu$, [443.90] | brown | 79 | >300 | 54.43 (54.11) | 3.87 (3.63) | 6.16 (6.31) | 14.05 (14.31) | 12 |
| **CuRCT** | $C_{20}H_{17}N_2O_{6.5}Cu$, [452.90] | Brown | 72 | >300 | 52.86 (53.04) | 3.77 (3.78) | 6.31 (6.18) | 14.26 (14.03) | 11 |
| **CuH** | $C_{24}H_{22}N_2O_{10}Cu_2$, [625.53] | Brown | 72 | >300 | 46.00 (46.08) | 3.46 (3.54) | 4.29 (4.47) | 20.51 (20.31) | 75 |
| **CuHCT** | $C_{24}H_{22}N_2O_{10}Cu_2$, [625.53] | Brown | 79 | >300 | 46.02 (46.08) | 3.77 (3.54) | 4.19 (4.47) | 20.05 (20.31) | 70 |

**Table S2**. Temperatures of decomposition and the kinetic parameters of complexes.

| Chelates | Step | n order | T (K) | A ($S^{-1}$) | Δ E (kJ $mol^{-1}$) | ΔH (kJ $mol^{-1}$) | ΔS (kJ $mol^{1}$ $K^{-1}$) | ΔG (kJ $mol^{-1}$) |
|---|---|---|---|---|---|---|---|---|
| **CuR** | First | 1 | 540 | $1.34x10^{9}$ | 97.51 | 93.02 | -0.835 | 138.15 |
| | Second | 0.33 | 672 | $2.55x10^{8}$ | 29.43 | 23.84 | -0.099 | 90.39 |
| **CuH** | First | 0.33 | 567 | $1.16x10^{11}$ | 13.88 | 9.17 | -0.046 | 35.25 |
| | Second | 0.5 | 635 | $2.95x10^{5}$ | 69.20 | 63.92 | -0.155 | 162.16 |
| **CuHCT** | First | 0 | 450 | $5.72x10^{9}$ | 14.43 | 10.68 | -0.069 | 42.12 |
| | Second | 1 | 562 | $7.06x10^{6}$ | 42.69 | 38.02 | -0.127 | 109.60 |
| **CuRCT** | First | 1 | 345 | $8.72\ x10^{9}$ | 64.85 | 61.98 | -0.064 | 84.06 |
| | Second | 0 | 590 | $3.81\ x10^{7}$ | 34.83 | 29.92 | -0.113 | 96.59 |
| | Third | 0.66 | 598 | $2.88x10^{6}$ | 77.82 | 72.85 | -0.135 | 153.58 |

**Table S3.** Characteristic IR spectral data of the **HCBH** and its copper nano-chelates.

| **Compound** | **IR spectral bands ($cm^{-1}$)** | | | | | | |
|---|---|---|---|---|---|---|---|
| | **υ(OH /$H_2O$)** | **υ(C-H)** | **υ(C=O) lactone** | **υ(C=N)** | **υ(M-O)** | **υ(M-N)** | **Additional bands** |
| **HCBH** | 3469 | 3041 | 1724 | 1572 | - | - | - |
| **CuR** | 3419 | 3048 | 1694 | 1560, 1510 | 555, 514 | 454 | 1487, **$\upsilon_{as}$**$(COO^{-})$1256, **$\upsilon_{s}$$(COO^{-})$ (Monodentate $oAc^{-}$)** |
| **CuRCT** | 3411 | 3054 | 1694 | 1560, 1512 | 585, 539 | 451 | 1486, **$\upsilon_{as}$**$(COO^{-})$1255, **$\upsilon_{s}$$(COO^{-})$ (Monodentate $oAc^{-}$)** |
| **CuH** | 3377 | 3046 | 1693 | 1550, 1520 | 575, 539 | 433 | 1478, **$\upsilon_{as}$**$(COO^{-})$1301, **$\upsilon_{s}$$(COO^{-})$ (bidentate $oAc^{-}$)** |
| **CuHCT** | 3377 | 3046 | 1693 | 1555, 1510 | 583, 540 | 450 | 1434, **$\upsilon_{as}$**$(COO^{-})$1313, **$\upsilon_{s}$$(COO^{-})$ (bidentate $oAc^{-}$)** |

**Table S4.** Quantum chemical parameters of **HCBH** and its copper chelates

| Compound | $E_{HOMO}$ | $E_{LUMO}$ | ΔE | IP | EA | χ | μ | η | σ | ω |
|---|---|---|---|---|---|---|---|---|---|---|
| **HCBH** | -6.26 | -2.24 | 4.02 | 6.26 | 2.24 | 4.25 | -4.25 | 2.01 | 0.25 | 4.49 |
| **CuR/CuRCT** | -8.83 | -5.98 | 2.84 | 8.83 | 5.98 | 7.40 | -7.40 | 1.42 | 0.35 | 19.27 |
| **CuH/CuHCT** | -8.22 | -5.60 | 2.62 | 8.22 | 5.60 | 6.91 | -6.91 | 1.31 | 0.38 | 18.23 |

**Table S5**. Hydrogen bonds between the studied compounds and the amino acids residues of the target protein (pdb ID: 3IG7).

| | Residual | Distance | Interaction | Binding energy (kcal/mol) |
|---|---|---|---|---|
| **HCBH** | HIS84 | 2.75 | Hydrogen Bond | -6.70 |
| | ASP145 | 4.78 | Pi-Anion | |
| | LYS89 | 4.20 | Pi-Alkyl | |
| **CuR/CuRCT** | LYS33 | 2.87 | Hydrogen Bond | -8.20 |
| | ASN132 | 2.86 | Hydrogen Bond | |
| | ASP145 | 3.01 | Hydrogen Bond | |
| | ASP86 | 2.55 | Pi-Anion | |
| | LYS88 | 4.60 | Pi-Alkyl | |
| | LYS33 | 4.32 | Pi-Alkyl | |
| **CuH/CuHCT** | LEU32 | 2.97 | Hydrogen Bond | -8.40 |
| | GLY11 | 2.83 | Hydrogen Bond | |
| | PHE80 | 4.08 | Pi-Pi | |
| | VAL18 | 4.06 | Pi-Alkyl | |
| | LYS33 | 4.94 | Pi-Alkyl | |
| | VAL18 | 5.45 | Pi-Alkyl | |
| | VAL18 | 4.51 | Pi-Alkyl | |
| | ALA31 | 4.00 | Pi-Alkyl | |

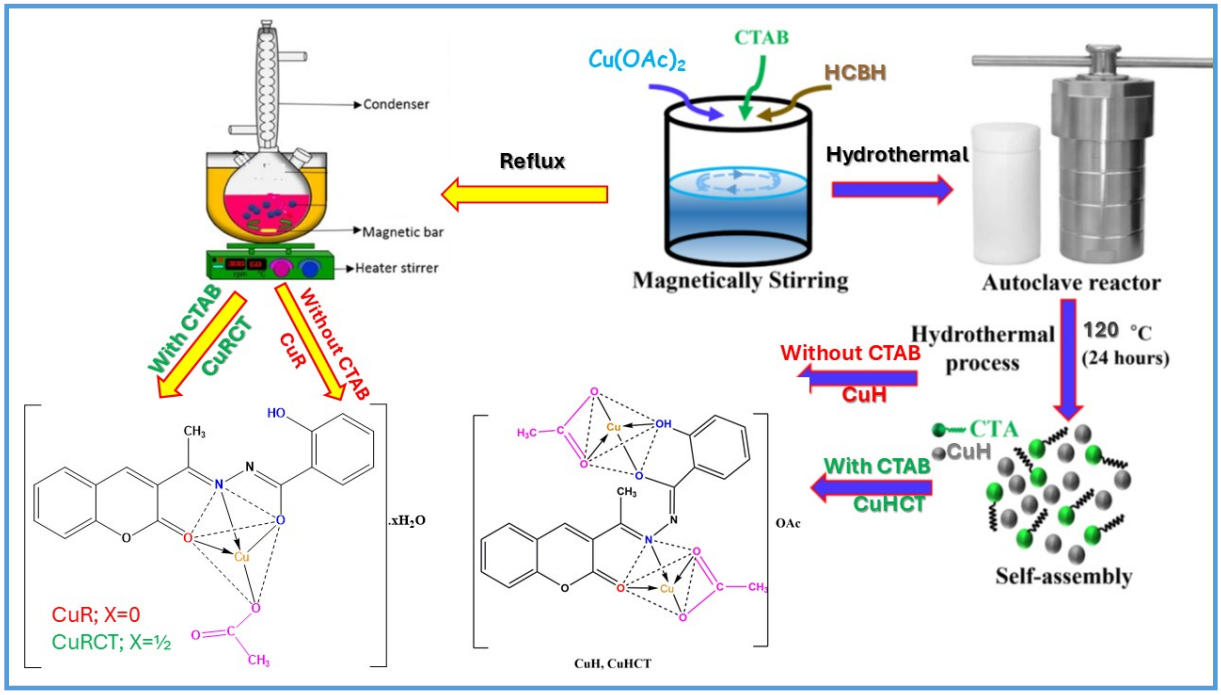


**Scheme S1.** Schematic representation of copper nano-chelate.

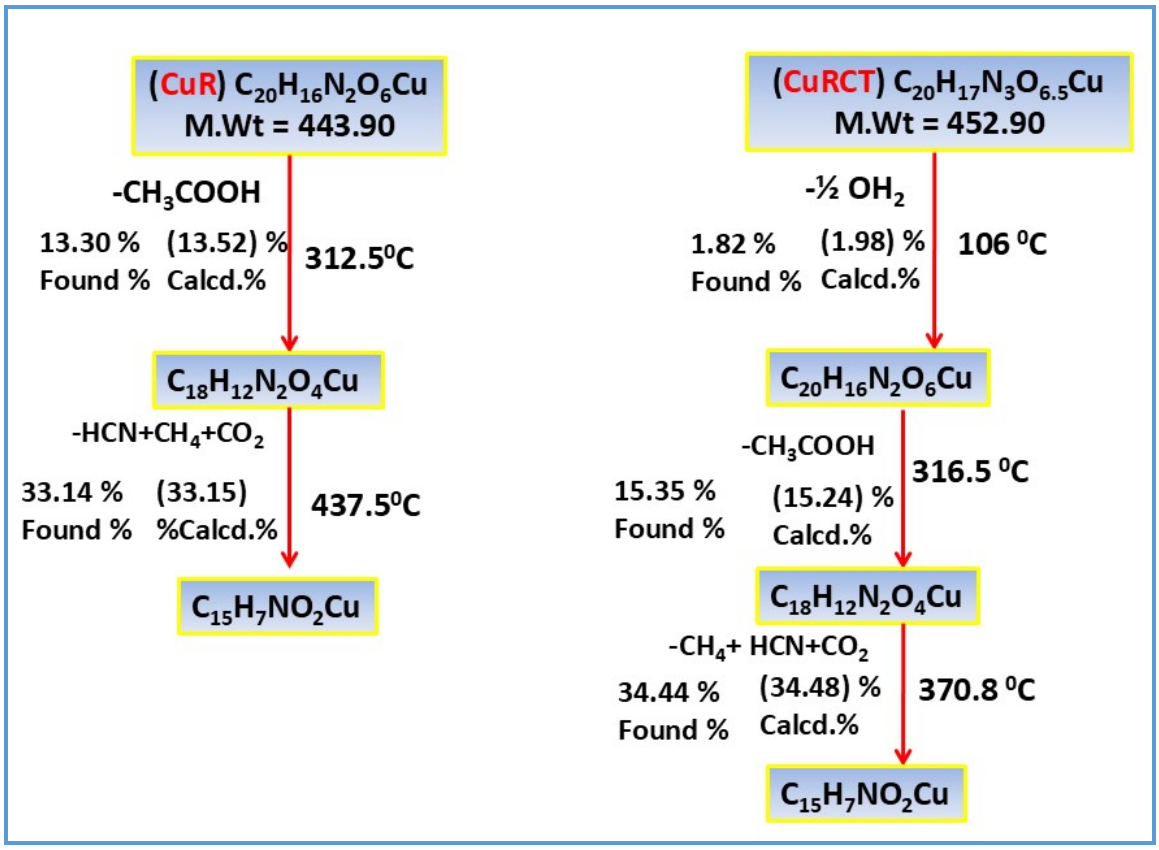


**Scheme S2.** Schematic representation of thermal degradation of **CuR**, and **CuRCT** chelates.

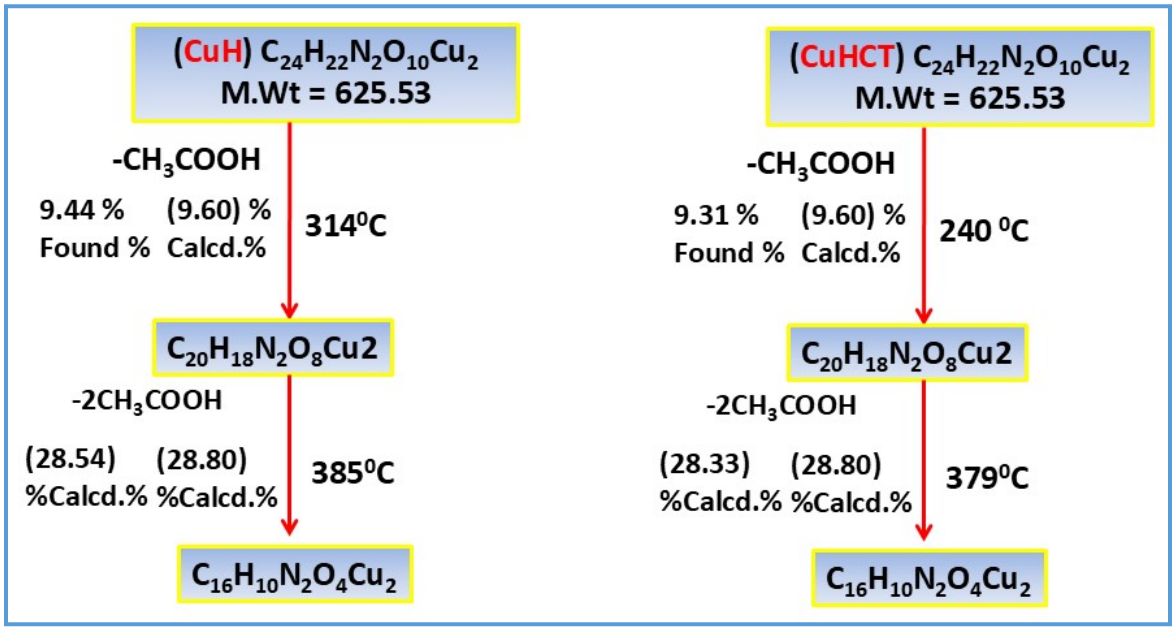


**Scheme S3.** Schematic representation of thermal degradation of **CuH**, and **CuHCT** chelates.

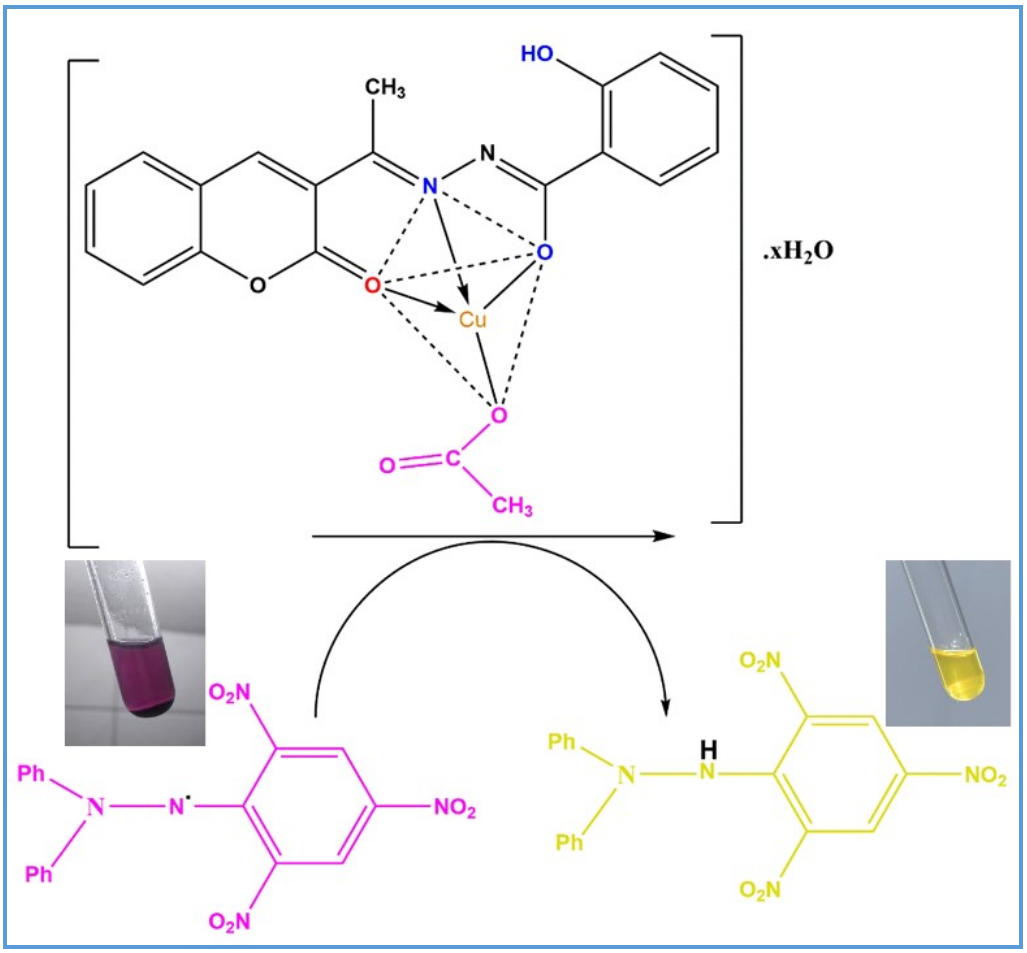


**Scheme S4.** The schematic representation of the color change of DPPH from purple to yellow after mixing with copper nano-chelate.